water

MDPI

Article

Evaluation of Evapotranspiration Prediction for Cassava Crop Using Artificial Neural Network Models and Empirical Models over Cross River Basin in Nigeria

Oluwadamilare Oluwasegun Eludire [1,2], Oluwaseun Temitope Faloye [3,4,*], Michael Alatise [2], Ayodele Ebenezer Ajayi [2,4,5], Philip Oguntunde [2], Tayo Badmus [1], Abayomi Fashina [6], Oluwafemi E. Adeyeri [7,*], Idowu Ezekiel Olorunfemi [8] and Akinwale T. Ogunrinde [9]

1 Department of Agricultural and Bioresources Engineering, Faculty of Engineering and Technology, University of Calabar, Calabar PMB 1115, Nigeria
2 Department of Agricultural and Environmental Engineering, Federal University of Technology, Akure PMB 704, Nigeria
3 Department of Water Resources Management and Agrometeorology, Federal University, Oye-Ekiti PMB 373, Nigeria
4 Institute for Plant Nutrition and Soil Science, Christian Albrecht's University zu Kiel, Hermann Rodewaldstr. 2, 24118 Kiel, Germany
5 Institute for Fourth Industrial Revolution, SE Bogoro Centre, Afe Babalola University, Ado Ekiti 360001, Nigeria
6 Department of Soil Science and Land Resources Management, Federal University, PMB 373, Oye-Ekiti 371104, Nigeria
7 School of Energy and Environment, City University of Hong Kong, Kowloon, Hong Kong
8 Department of Civil Engineering, Lead City University Ibadan, Ibadan 200255, Nigeria
9 Key Laboratory of Ecological Safety and Sustainable Development in Arid Lands, Northwest Institute of Eco-Environment and Resources, Chinese Academy of Sciences, Beijing 100045, China
* Correspondence: oluwaseun.faloye@fuoye.edu.ng (O.T.F.); cyndyfem@gmail.com (O.E.A.)

Abstract: The accurate assessment of water availability throughout the cassava cropping season (the initial, developmental, mid-season, and late stages) is crucial for mitigating the impacts of climate change on crop production. Using the Mann–Kendall Test, we investigated the trends in rainfall and cassava crop evapotranspiration (ETc) within the Cross River basin in Nigeria. Reference evapotranspiration (ETo) was based on two approaches, namely Artificial Neural Network (ANN) modelling and three established empirical models—the Penman–Monteith (considered the standard method), Blaney–Morin–Nigeria (BMN), and Hargreaves–Samani (HAG) models. ANN predictions were performed by using inputs from BMN and HAG parameters, denoted as BMN-ANN and HAG-ANN, respectively. The results from the ANN models were compared to those obtained from the Penman–Monteith method. Remotely sensed meteorological data spanning 39 years (1979–2017) were acquired from the Climatic Research Unit (CRU) to estimate ETc, while cassava yield data were acquired from the International Institute of Tropical Agriculture (IITA), Ibadan. The study revealed a significant upward trend in cassava crop ETc over the study period. Additionally, the ANN models outperformed the empirical models in terms of prediction accuracy. The BMN-ANN model with a Tansig activation function and a 3-3-1 architecture (number of input neurons, hidden layers, and output neurons) achieved the highest performance, with a coefficient of determination (R^2) of 0.9890, a root mean square error (RMSE) of 0.000056 mm/day, and a Willmott's index of agreement (d) of 0.9960. There is a decreasing trend in cassava yield in the region and further analysis indicated potential average daily water deficits of approximately −1.1 mm/day during the developmental stage. These deficits could potentially hinder root biomass, yield, and overall cassava yield in the Cross River basin. Our findings highlight the effectiveness of ANN modelling for irrigation planning, especially in the face of a worsening climate change scenario.

Academic Editor: Guangyuan Kan

Received: 28 August 2024
Revised: 5 October 2024
Accepted: 8 October 2024
Published: 1 January 2025

Citation: Eludire, O.O.; Faloye, O.T.; Alatise, M.; Ajayi, A.E.; Oguntunde, P.; Badmus, T.; Fashina, A.; Adeyeri, O.E.; Olorunfemi, I.E.; Ogunrinde, A.T. Evaluation of Evapotranspiration Prediction for Cassava Crop Using Artificial Neural Network Models and Empirical Models over Cross River Basin in Nigeria. *Water* **2025**, *17*, 87. https://doi.org/10.3390/w17010087

Keywords: artificial neural networks (ANN); irrigation; cassava crop evapotranspiration; Cross River basin; neuron; modelling; FAO-56 Penman–Monteith model; climate change

1. Introduction

Evapotranspiration (ET) is a simultaneous process involving water loss from the soil surface through evaporation and from leave surfaces through transpiration. About 62% of precipitation recorded on the Earth's surface is returned to the atmosphere through evapotranspiration [1]. In the hydrologic cycle, evapotranspiration plays a vital role in various fields of water resources, especially in determining the crop water requirement for irrigation planning. A prominent method for estimating crop evapotranspiration (ETc) is to predict the reference evapotranspiration (ETo) and multiply it by the suitable crop coefficient (kc), respectively [2]. The United Nations Food and Agricultural Organization (FAO) defines calculating ETo using a hypothetic crop of uniform height (12 cm), that is actively developing (crop resistance of 70 sm^{-1}), that completely covers the surrounding soil (albedo of 0.23), and with an unrestricted water supply [3]. The definition is regarded as a standard method for estimating ETo if relevant climatic data are accessible [2,4]. The estimation of ETo is complex due to the nonlinearity between various climatic variables (wind speed, maximum and minimum air temperature, and maximum and minimum relative humidity solar radiation) and ETo. However, there are direct and indirect methods of measuring ETo, but some of these methods have limitations with respect to the availability of reliable data, which is affecting the accurate estimation of crop evapotranspiration (ETc) in important crops, including cassava [5].

Cassava is a tropical root crop and forms one of the basic sources of daily dietary energy for more than 500 million people globally [6], due to its starch content. It is usually sold as a processed product in the form of gari, fufu, and flour [7]. The cultivation of cassava in Cross River basin largely depends on rain-fed systems, which have reduced the farmers yield and earnings [8]. However, recent studies have indicated that the yield and production of cassava have experienced a decreasing trend in the Cross River basin over the years due to rainfall deficits during the cropping season [9]. Therefore, this has necessitated the accurate estimation of the water requirements of cassava at different cropping stages.

Studies comparing ANN, Penman–Monteith (PM), and empirical methods with limited climatic data are scarce, particularly for the Hargreaves–Samani (HAG) and Blaney–Morin–Nigeria (BMN) models, which the Nigerian Institution of Agricultural Engineers (NIAE) consider to be best suited for the Nigerian climate, as developed by Duru [10]. Also, assessing the long-term trend in the crop evapotranspiration of cassava is important, since it would enable the estimation of the rainfall deficit or surplus during the cassava cropping season, which is important for rain-fed crops like cassava in the Cross River basin [11]. Therefore, the accurate ETo prediction of cassava in the Cross River Basin is critical for a better yield. The specific objectives of this research are as follows: (i) to assess rainfall trends during the cassava cropping season; (ii) to predict reference evapotranspiration and estimate cassava crop evapotranspiration (ETc) in the Cross River basin using empirical (PM, BMN, and HAG) and ANN models; and (iii) to accurately estimate the surplus or deficit water requirement of cassava in the Cross River basin.

2. Materials and Methods

2.1. Study Area

The Cross River basin is one of river basins accommodating the Akwa Ibom and Cross River states as a catchment in the south–south geopolitical zone of Nigeria. The Cross

River basin is located between latitudes 4°00′ N and 6°50′ N and longitudes 7°40′ E and 90°40′ E. It is characterized by high rainfall (which ranges between 1250 mm and 4000 mm per annum); temperature (between 22 °C and 30 °C); and high relative humidity [11]. Figure 1 shows the geographical location of the Cross River basin, as well as the names of the 22 climatic stations within the basin.

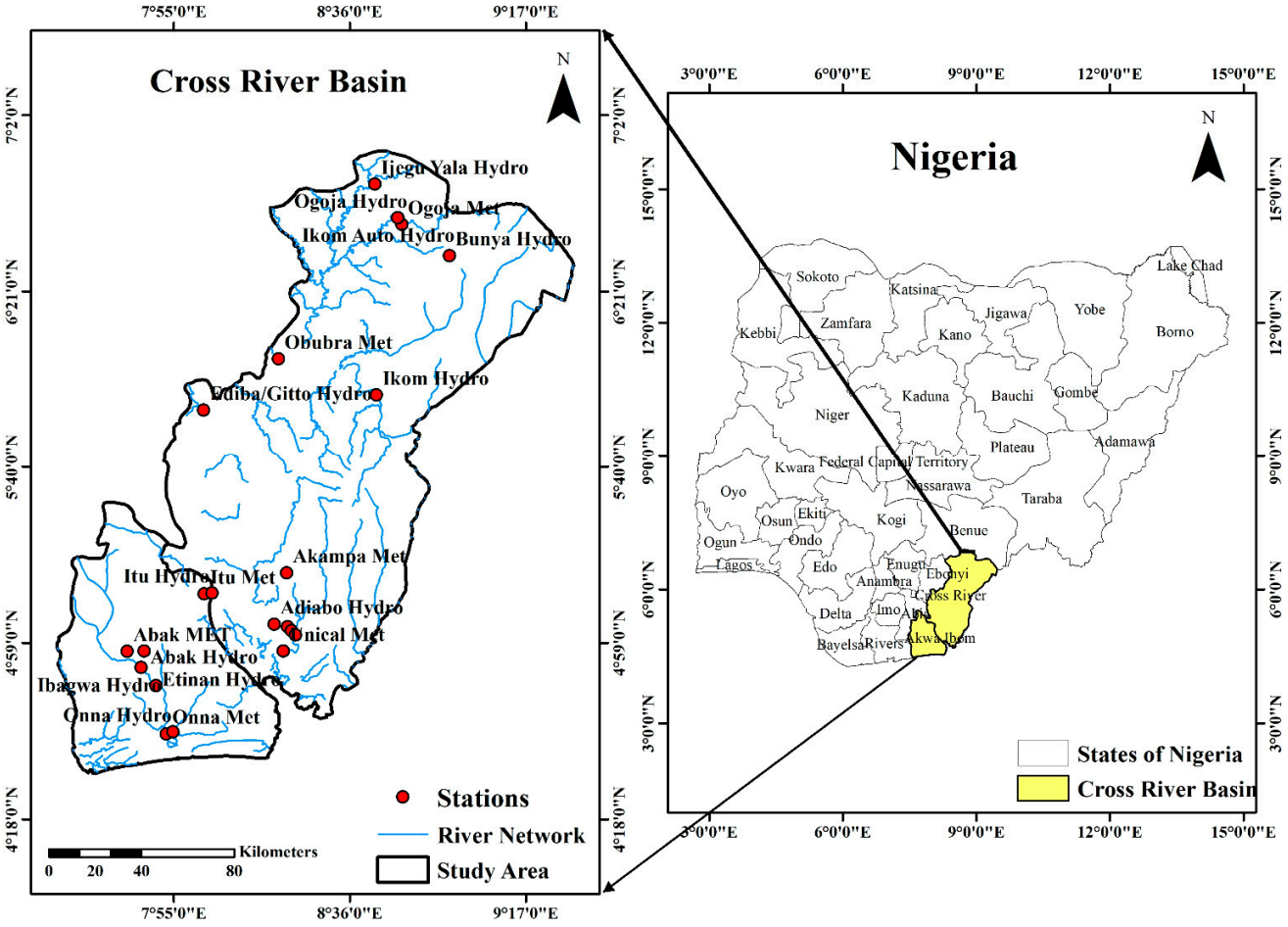

Figure 1. Map of Nigeria showing the Cross River basin, showing the 22 stations used by ArcGIS Pro 3.1.

2.2. Climatic Data and Partitioning

For this study, 22 meteorological stations were selected with respect to the recommendation of the Cross River Basin Development Authority (CRBDA) of Nigeria. Remotely sensed climatic data; minimum air temperature (Tmin); maximum air temperature (Tmax); mean relative humidity (RH); solar radiation (Sr) means; wind speed (Ws); and rainfall (R) ranging from the year 1979 to 2017 were obtained from the Climatic Research Unit (CRU) of the University of East Anglia, Norwich, United Kingdom.

The data were detailed on a monthly and annual basis, as well as in relation to the cropping season of cassava, as recommended by Akpan et al. [12], for 39 years (1979–2017). In total, 70% of the data for ETo prediction were selected for ANN training, 15% were used for ANN validation, and the other 15% were used for ANN testing, which was adopted from Sarangi et al. [13].

2.3. Temporal Analysis of Rainfall over Cross River Basin

The trend analysis of rainfall over the basin was performed with the obtained 1979–2017 data by the use of a Mann–Kendall test. The test was carried out on a monthly, seasonal, and annual basis.

Mann–Kendall Test

The Mann–Kendall test, which was developed by Mann [14] and Kendall [15], was used in this study due to its advantage in detecting linear or nonlinear trends [16,17]. It is a non-parametric method for trend analysis and is used for analyzing temporal trends in climatology and hydrology time series data [18]. The null and alternate hypotheses were tested at the 0.1, 0.05, 0.01, and 0.001 significance levels, while the related equations for conducting the Mann–Kendall (MK) test statistic (S), variance of statistics (S) (Var(S)), and the standardized test statistic (ZMK) are shown in Equations (1)–(4).

$$S = \sum_{i=1}^{n} \sum_{j=i+1}^{n-1} sgn(X_j - X_i) \quad (1)$$

$$sgn(X_j - X_i) = \begin{Bmatrix} +1 & if & (X_j - X_i) > 0 \\ 0 & if & (X_j - X_i) = 0 \\ -1 & if & (X_j - X_i) < 0 \end{Bmatrix} \quad (2)$$

$$Var(S) = \frac{1}{18}\left[n(n-1)(2n+5) - \sum_{p=1}^{q} t_p(t_p-1)(2t_p+5)\right] \quad (3)$$

$$Z_{MK} = \begin{cases} \frac{S-1}{\sqrt{Var(S)}} & if \quad S > 0 \\ 0 & if \quad S = 0 \\ \frac{S+1}{\sqrt{Var(S)}} & if \quad S < 0 \end{cases} \quad (4)$$

where X_i and X_j are the sequential data values of the time series in the years i and j, n is the length of the time series, tp is the number of ties for the probability value, and q is the number of tied values. Positive values of Z_{MK} indicate increasing trends, while negative Z_{MK} values indicate decreasing trends in the time series. When $|Z_{MK}| > Z_{(1-\alpha/2)}$, the null hypothesis is rejected and a significant trend exists in the time series. $Z_{(1-\alpha/2)}$ is the critical value of Z from the standard normal table; the tested significance levels α are 0.001, 0.01, 0.05, and 0.l.

2.4. Experimental Procedure

The adopted cropping season for cassava spans from November to June (210 days). These planting days include the initial stage, developmental stage, mid-season, and late season, as highlighted in the FAO's Irrigation and Drainage Paper No. 56. The respective duration in days used in this study are as follows: Lini (20 days), Ldev (40 days), Lmid (90 days), and Llate (60 days), according to Allen et al. [2]. Akpan and Udoh [12] posited in their investigation that the period between June and October is the peak rainfall over the Cross River basin. Therefore, the period between November and June were adopted as a suitable cassava cultivation season to avoid the seasonal flooding commonly experienced in the basin. The Kc values in this study were localized by the use of Equations (5) and (6), according to Allen et al. [2]. The Kc ini of 0.3 was adopted for the initial stage, according to Allen et al. [2], since it a constant value. The crop coefficients—Kc mid for mid-season and Kc end for late season—were computed by the use of Equations (5) and (6), where the mean crop height within the area of study was obtained from a previous study [19]. The numerical determination of the crop coefficient Kc of cassava was performed to determine Kci during the developmental stage and late season by the use of Equation (7); these and

the localized crop coefficient Kc of cassava over the Cross River basin are expressed in Table 1.

$$K_{cmid} = K_{cmid\ (Tab)} + [0.04(U_2 - 2) - 0.004(RH_{min} - 45)]\left(\frac{h}{3}\right)^{0.3} \quad (5)$$

where Kc mid $_{(Tab)}$ is taken from Allen et al. [2]; U_2 is the mean value of daily wind speed at a 2 m height over the grass during the midseason growth stage [m.s^{-1}]; RH_{min} is the mean value for daily minimum relative humidity during the mid-season growth stage [%], for 20% $\leq RH_{min} \leq$ 80%; and h is the mean plant height during the mid-season stage [m].

$$K_{cend} = K_{cend(tab)} + [0.04(U_2 - 2) - 0.004(RH_{min} - 45)]\left(\frac{h}{3}\right)^{0.3} \quad (6)$$

where Kc end $_{(Tab)}$ is taken from Allen et al. [2]; U_2 is the mean value for daily wind speed at a 2 m height over the grass during the late growth stage [m.s^{-1}]; RH_{min} is the mean value for daily minimum relative humidity during the late growth stage [%], for 20% $\leq RH_{min} \leq$ 80%; and h is the mean plant height during the late season [m].

$$K_{ci} = K_{cprev} + \left[\frac{i - \sum(L_{prev})}{L_{stage}}\right](K_{cnext} - K_{cprev}) \quad (7)$$

where i is the day number under consideration within the cropping season (1. length of the growing season); K_{ci} is the crop coefficient on day i; K_{cprev} is the previous crop coefficient before day i under consideration; L_{stage} is the length of the stage under consideration in days; and $\Sigma(L_{prev})$ is the sum of the lengths of all previous stages in days.

Table 1. Localized crop coefficient (K_c) values of cassava.

Growth Stages (Days After Planting)	Kc
Initial Stage (1–20)	0.3
Developmental Stage (21–60)	0.31–0.69
Mid-Season (61–150)	0.69
Late Season (151–210)	0.68–0.13

2.5. The Calculation Procedure for Crop Evapotranspiration (ETc) of Cassava

Crop evapotranspiration (ETc) was calculated as the multiplication of ETo from ANN models and empirical models using crop coefficients [10]. The ETc values were compared at each corresponding stage of the cropping season. The Etc is computed from the Penman–Monteith [2], Blaney–Morin–Nigeria [10], and Hargreaves–Samani Models [20], as illustrated in Equations (8)–(11).

Penman–Monteith model (P-M):

$$ET_O = \frac{0.408\Delta(R_n - G) + \gamma\frac{900}{(T+273)}u_2(e_s - e_a)}{\Delta + \gamma(1 + 0.34u_2)} \quad (8)$$

where ETo is the reference evapotranspiration [mm d^{-1}], R_n is the net radiation at the crop surface [MJm^{-2} day^{-1}], G is the soil heat flux density [MJm^{-2} d^{-1}], T is the mean daily air temperature at a 2 m height [°C], u_2 is the wind speed at a 2 m height [ms^{-1}], es is the saturation vapour pressure [kPa], e_a is the actual vapour pressure [kPa], $e_s - e_a$ is the saturation vapour pressure deficit [kPa], Δ is the slope vapour pressure curve [kPa °C^{-1}], and γ is the psychrometric constant [kPa °C^{-1}].

Blaney–Morin–Nigeria (BMN):

$$ET_o = r_f(0.45Ta + 8)\left(520 - R^{1.31}\right)/100 \quad (9)$$

where ETo is the reference crop evapotranspiration (mm d^{-1}), rf is the ratio of monthly radiation to annual radiation, Ta is the mean monthly temperature in °C, and R is the mean monthly relative humidity.

Hargreaves–Samani model (HAG):

$$ET_O = (0.0023)R_a(T + 17.8)TD^{0.5} \quad (10)$$

where ETo is the reference crop evapotranspiration (mm d^{-1}), Ra is the extra-terrestrial solar radiation received on the Earth's surface (mm d^{-1}), TD is the difference in mean maximum and minimum air temperatures (°C), and T is the mean air temperature (°C).

Crop evapotranspiration of cassava (ETc):

$$ET_C = K_C \times ET_O \quad (11)$$

where ET_c is the crop evapotranspiration (mm d^{-1}), ET_o is the reference evapotranspiration (mm d^{-1}), and K_c is the crop coefficient.

2.6. Artificial Neural Network Modelling Strategy

2.6.1. Data Preparation and Normalization

Datasets were arranged with respect to the climatic variables required in the Blaney–Morin–Nigeria (BMN) and Hargreaves–Samani (HAG) models. Data normalization was carried out to readjust the inputs and target them in a way that they fall within a range of 0 and +1 for the Logsigmoid (LOGSIG) transfer function and −1 and +1 for the Tansigmoid (TANSIG) transfer function. These functions help to derive the output from the input datasets fed into the hidden layer(s); these functions are characterized by their high aptitude to simulate extreme data and speed, respectively [21].

2.6.2. Artificial Neural Network Model

Artificial Neural Network modelling for estimating the crop evapotranspiration (ETc) of cassava was carried out using the MATLAB R2017a Neural Network toolbox. The Feed-Forward Back Propagation (FFBP) algorithm was adopted because it is characterized by a good performance in hydrologic-related studies [22]. ANN TRAINLM is a training function that predicts the outputs and updates the network weight in line with the Levenberg–Marquardt optimization; it is one of the fastest back propagation algorithms [23]. This ANN modelling was performed using the LEARNGDM learning function, which means gradient descent with momentum weight and bias learning function. Learning is a process through which a neural network adapts itself to a stimulus by making proper parameter adjustments, producing the desired results.

2.6.3. ANN Modelling Strategy and Architecture

Developing an ANN model for hydrological modeling lacks a universal set of guidelines. However, successful applications in the field can serve as a foundation for building a specific framework. The typical ANN structure consists of three layers—an input layer that receives normalized climatic variables, one or more hidden layers that perform nonlinear transformations on the data, and an output layer that delivers the desired predictions. Information processing within the network follows a forward direction, layer by layer. This study employed a three-layer architecture, with one hidden layer and a final output layer,

as shown in Figure 2. It is important to note that the input layer and its parameters are not typically counted as a layer in the model. The optimal number of hidden neurons is often determined through a trial-and-error process during model training and can range from 1 to 3 [24]. Our specific ANN configuration utilized three input parameters—the Feed-Forward Back propagation (FFBP) algorithm and two transfer functions (logistic sigmoid and tan-sigmoid). The Neural Networks toolbox determined the reported number of epochs used for training the neural networks. Subsequently, the normalized dataset (totaling 1404 data points) was divided into three groups—70% (982 data points) for training, 15% (211 data points) for validation, and another 15% (211 data points) for testing the performance of the ANN model for each architecture.

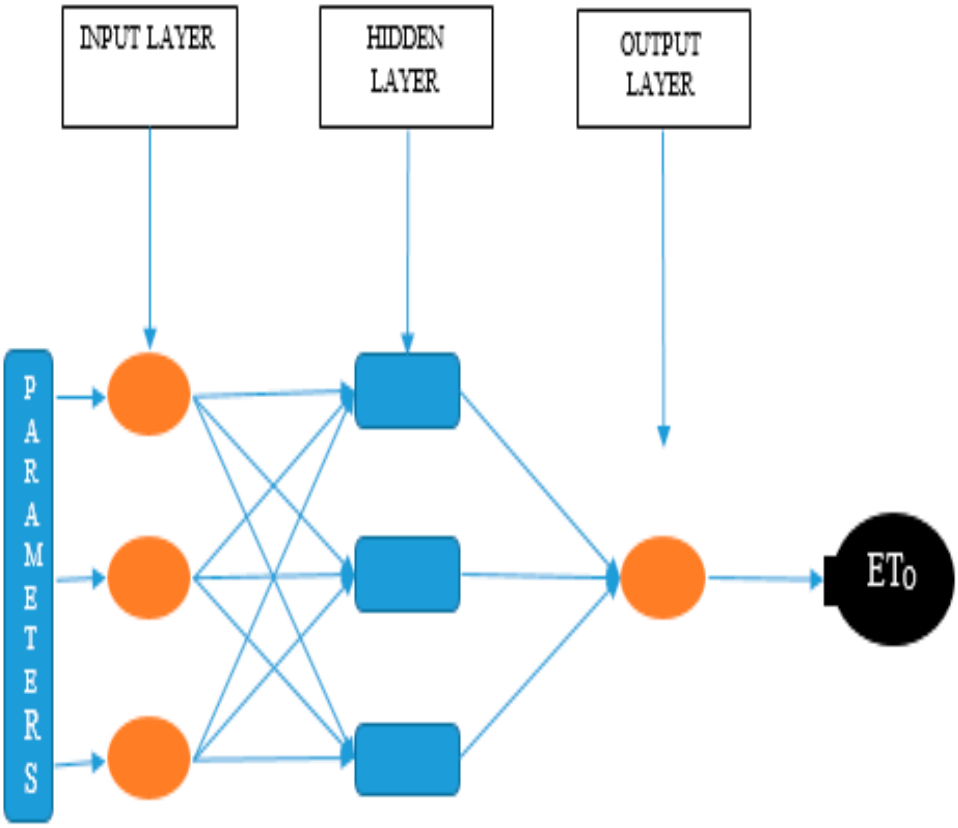

Figure 2. Network architecture showing input, hidden, and output layer connections.

2.6.4. ANN Modelling Strategies

This study employed two ANN modeling strategies. Both strategies utilized three normalized climatic variables as inputs, corresponding to the Blaney–Morin–Nigeria (BMN) and Hargreaves–Samani (HAG) models [20] (details provided in Table 2). The FFBP algorithm was chosen to train the networks. Additionally, two separate transfer functions were evaluated for each strategy—the TANSIG (tangent sigmoid) and LOGSIG (logistic sigmoid) functions. Therefore, BMN-LogSig-ANN-3-1-1 can be expressed as as ANN modelling strategy with three Blaney–Morin–Nigeria input parameters, one hidden layer neuron, and one output layer.

Table 2. Artificial Neural Network (ANN) model architecture.

Feed Forward Back Propagation (FFBP)			
Transfer Functions	**Hidden Layer Neuron(s)**	**Input Parameters (Strategies)**	
		BMN	**HAG**
LOGSIG	1	BMN-Logsig-ANN	HAG-Logsig-ANN
	2	BMN-Logsig-ANN	HAG-Logsig-ANN
	3	BMN-Logsig-ANN	HAG-Logsig-ANN
TANSIG	1	BMN-Tansig-ANN	HAG-Tansig-ANN
	2	BMN-Tansig-ANN	HAG-Tansig-ANN
	3	BMN-Tansig-ANN	HAG-Tansig-ANN

2.6.5. Performance Evaluation of Models

Root Mean Square Error (RMSE)

This is a measure of the accuracy of the model and it is simply described as the square root of the mean square error. The advantage of using RMSE is that RMSE has the same units as that of the variables involved in the computation [25]. It is calculated as follows:

$$RMSE = \sqrt{\frac{1}{N}\sum_{i=1}^{N}\left(ETi_{obs} - ETi_{pred}\right)^2} \quad (12)$$

where ETi_{obs} is the observed reference evapotranspiration (mm/d), ETi_{pred} is the empirical or ANN models' predicted evapotranspiration (mm/d), and N is the total amount of evapotranspiration data considered.

Coefficient of Determination (R^2)

The coefficient of determination is a standard measure of goodness-of-fit for mathematical models fitted to empirical data by means of least squares regression; it is a measure of the precision of the prediction model [26], and it is calculated as follows:

$$R^2 = \left(\frac{\frac{1}{N}\sum_{i=1}^{N}\left[ETi_{obs} - MET_{obs}\right]\left[ETi_{pred} - MET_{pred}\right]}{\sqrt{\frac{1}{N}\sum_{i=1}^{N}\left(ETi_{obs} - MET_{obs}\right)^2}\sqrt{\frac{1}{N}\sum_{i=1}^{N}\left(ETi_{pred} - MET_{pred}\right)^2}}\right)^2 \quad (13)$$

where MET_{obs} is the arithmetic mean of the observed evapotranspiration (mm/d), and MET_{pred} is the arithmetic mean of the predicted evapotranspiration (mm/d).

Willmott Index of Agreement (d)

This is the degree of model prediction error; it ranges between 0 and 1. The index of agreement denotes the relationship between the mean square error and the potential error. An agreement value of 1 indicates an accurate match, while a value of 0 indicates that there is no agreement. The index of agreement can sense additive and proportional variation in the observed and predicted values [27].

$$d = 1 - \frac{\sum_{i=1}^{n}\left(O_i - P_i\right)^2}{\sum_{i=1}^{n}\left(\left|P_i - O_m\right| + \left|O_i - O_m\right|\right)^2} \qquad 0 \le d \le 1 \quad (14)$$

where O_i is the observation value, P_i is the predicted value, and O_m is the average observation value.

3. Results and Discussion

3.1. Descriptive Statistics of the Climatic Parameters of Cross River Basin (1979–2017)

A summary of the relevant meteorological parameters used for the computation of crop evapotranspiration is shown in Table 3. The temperature range reported is in

agreement with the findings of Ewona and Udo [28], who posited that the average values of the minimum and maximum temperature over Cross River basin range between 21.8 °C and 31.5 °C. Table 3 summarizes the relevant meteorological variables used to calculate crop evapotranspiration.

Table 3. Descriptive statistics of climatic parameters of Cross River basin (1979–2017).

Climatic Variables	Minimum Value	Maximum Value	Mean Value	Standard Deviation
Solar Radiation (MJ/m^2/day)	18.23	23.33	20.76	1.0266
Wind Speed (m/s)	0.00	3.23	0.89	0.5714
Minimum Temperature (°C)	17.60	24.60	22.00	1.0390
Maximum Temperature (°C)	27.00	36.70	31.13	1.8234
Relative Humidity (%)	16.81	92.85	82.04	10.7242
Extra Terrestrial Radiation (mm/day)	12.65	15.47	14.49	0.9679
Rainfall (mm)	0.00	181.00	6.51	16.05

Table 4 presents the rainfall characteristics of the Cross River basin. The average annual rainfall from 1979 to 2017 was 2223.94 mm, with a standard deviation of 148.92 mm. The coefficient of variation (CV) was 6.7%, indicating a high precision in the annual rainfall data, according to Gomes [29]. Gomes [26] suggests that a CV less than 10% in field experiments signifies a high measurement precision. The highest rainfall occurred in September (350.7 mm), contributing 15.77% to the annual rainfall. August, July, and June followed in decreasing order, contributing 15.68%, 14.06%, and 12.77% to the annual rainfall, respectively. Notably, the cassava cropping season (November–June) receives 971.06 mm (42.53%) of the annual rainfall. January, February, and December experienced the least rainfall, contributing only 0.80%, 0.87%, and 1.60% to the annual rainfall, respectively. These months also exhibit the highest coefficients of variation (87.80%, 81.00%, and 70.80%, respectively). In contrast, May has the lowest CV (11.60%).

Table 4. Mean monthly, cropping season, and annual rainfall statistics of Cross River basin (1979–2017).

Month/Season	Rainfall (mm)	Standard Deviation	Coefficient of Variation (%)	% Contribution to Rainfall
January	17.7	15.5741	87.8	0.80
February	35.5	25.1666	70.8	1.60
March	108.3	31.4804	29.1	4.87
April	168.4	30.3872	18.0	7.57
May	236.8	27.4767	11.6	10.65
June	284.0	36.0122	12.7	12.77
July	312.6	80.239	25.7	14.06
August	348.8	49.7232	14.3	15.68
September	350.7	52.4313	15.0	15.77
October	261.6	49.5094	18.9	11.76
November	80.1	31.7745	39.7	3.60
December	19.5	15.7522	81.0	0.87
Cropping season	971.06	98.9229	10.5	43.66
Annual rainfall	2223.9	148.92	6.7	100.00

An analysis of the rainfall trends during the cassava cropping season (1980–2017) revealed a statistically significant increase (p-value = 0.01), as shown in Figure 3. This trend suggests gradual changes in rainfall patterns, potentially linked to climate change. These findings align with observations by Blenkinsop et al. [30], Sun et al. [31], and Donat et al. [32], who reported increasing global rainfall trends throughout the 20th and 21st centuries, affecting both dry and wet regions.

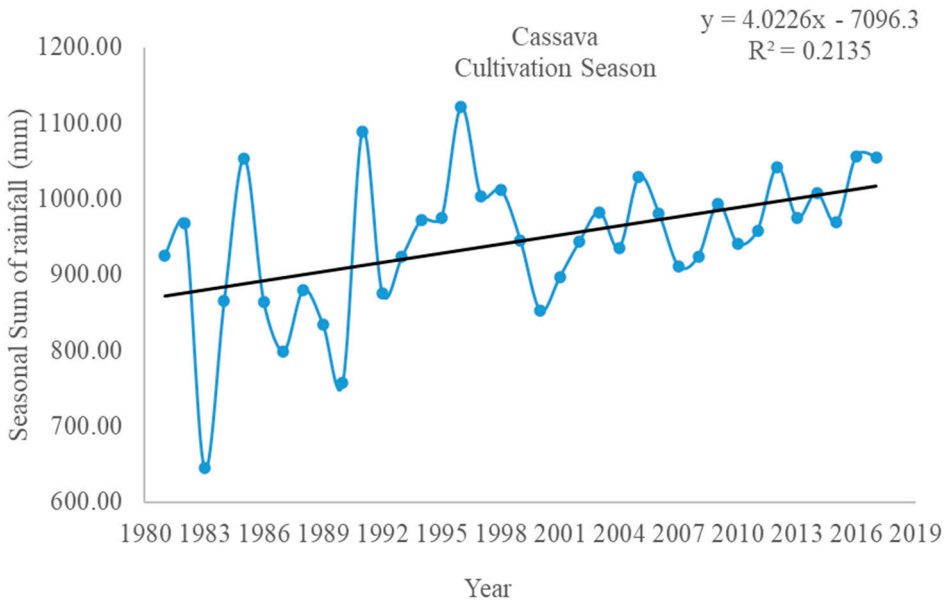

Figure 3. Annual trend in cassava cropping seasonal rainfall.

3.2. Temporal Analysis of Rainfall and Cassava Yield over Cross River Basin

The Mann–Kendall test results shown in Table 5 reveal trends in monthly rainfall during the cassava cropping season. Positive trends were observed in January and April, with statistical significance at the 0.1 confidence interval. However, February, March, June, September, and November exhibited positive trends that lacked statistical significance (p-value > 0.1). Conversely, May, August, and October displayed negative trends, although these were statistically insignificant at the 0.1 confidence interval. Notably, July experienced a significant negative trend (p-value = 0.001), while December showed a positive trend with significance at the 0.05 confidence interval. The annual rainfall and cassava yield data (2003–2017) obtained from International Institute of Tropical Agriculture (IITA), Ibadan, over the basin (Figure 4) exhibited a statistically significant negative trend (p-value = 0.1).

Table 5. Z-statistics of mean monthly, annual, and seasonal rainfall of Cross River basin.

Time Series	Test Z	Significance Level (%)
January	1.662755	90
February	1.406534	<90
March	0.763239	<90
April	1.871888	90
May	−0.667497	<90
June	1.573592	<90
July	−3.382046	99.9
August	−0.618951	<90
September	0.629806	<90
October	−0.351539	<90
November	0.278984	<90
December	2.331929	95
Cropping season	2.715531	99
Annual	−0.919362	<90
Cassava yield	−0.395897	<90

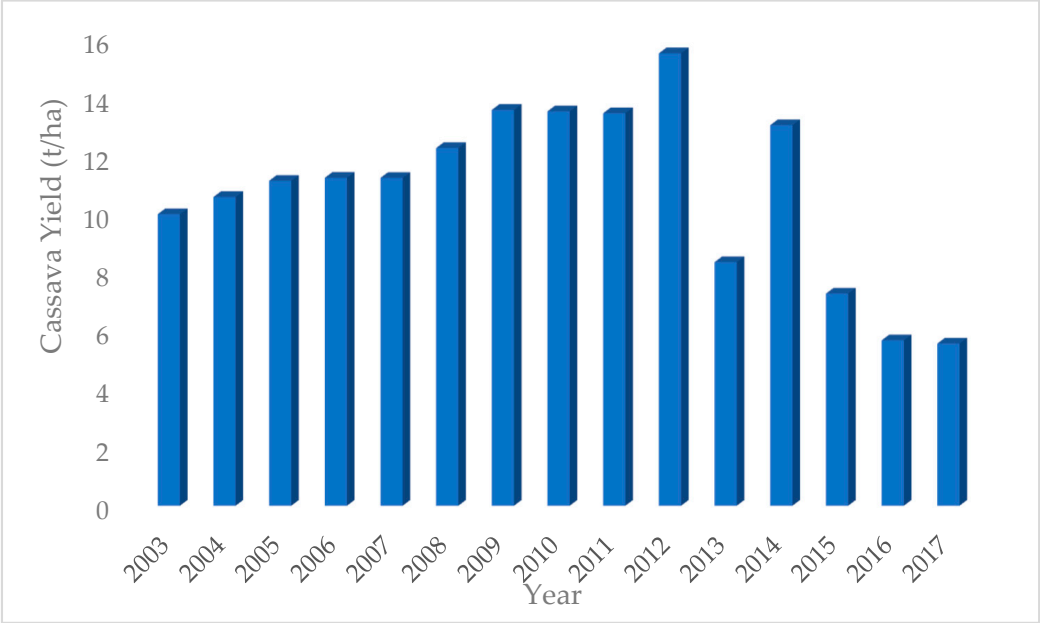

Figure 4. Annual yield of cassava over Cross River basin from IITA yield data.

3.3. Crop Evapotranspiration (ETc) of Cassava

Table 6 summarizes the estimated daily cassava crop evapotranspiration (ETc) using various models. The Penman–Monteith method (considered the standard method) yielded an average ETc of 2.2 mm/day, with variations across growth stages, namely 1.2 mm/day (initial), 1.9 mm/day (developmental), 2.9 mm/day (mid-season), and 1.8 mm/day (late season). The Blaney–Morin–Nigeria model produced a slightly lower average ETc (2.0 mm/day) with a similar seasonal pattern. The Hargreaves–Samani model, on the other hand, estimated a higher average ETc (2.6 mm/day) with a comparable seasonal distribution. Notably, the Penman–Monteith method displayed a coefficient of variation (CV) of 12.07%. These discrepancies between the empirical models (Blaney–Morin–Nigeria and Hargreaves–Samani) and the standard Penman–Monteith method highlight the importance of accurate water requirement estimation for cassava. This underscores the potential value of ANNs in providing more precise water use assessments compared to traditional empirical methods.

Table 6. Comparison of mean crop evapotranspiration (ETc) of cassava using empirical models (Penman–Monteith model, Blaney–Morin–Nigeria model, and Hargreaves–Samani model) over Cross River basin across the growth stages.

Growth Stages	Stage Length (Days)	Penman–Monteith (mm/d)	Blaney–Morin–Nigeria (mm/d)	Hargreaves–Samani (mm/d)	Coefficient of Variation (%)
Initial stage	20	1.2	0.9	1.3	16.34
Developmental stage	40	1.9	1.8	2.2	8.27
Mid-season	90	2.9	2.8	3.4	11.37
Late season	60	1.8	1.3	2.0	19.03
Total	210	2.2	2.0	2.6	12.07

3.4. Estimation of Reference Evapotranspiration and Crop Evapotranspiration of Cassava Using Log-Sigmoid (LOGSIG) and TANSIG Transfer Functions with the Parameters of the Blaney–Morin–Nigeria and Hargreaves–Samani Models

Examining reference evapotranspiration predictions using the LogSig transfer function (Table 7) revealed that the ANN model with the fewest neurons (BMN-LogSig-ANN-3-1-1) (Figure 5) achieved effective network training. Validation metrics demonstrate a

strong performance across all models, with R^2 values ranging from 0.8002 to 0.9880, RMSE values between 0.005076 mm/day and 0.000177 mm/day, and index of agreement 'd' values ranging from 0.9360 to 0.9960. Notably, the estimated daily cassava crop evapotranspiration (ETc) is approximately 2.3 mm/day, with variations across growth stages (1.2 mm/day for initial, 1.9 mm/day for developmental, 3.0 mm/day for mid-season, and 1.8 mm/day for late season). The BMN-LogSig-ANN-3-3-1 model's ETc estimates closely align with those obtained from the standard Penman–Monteith method.

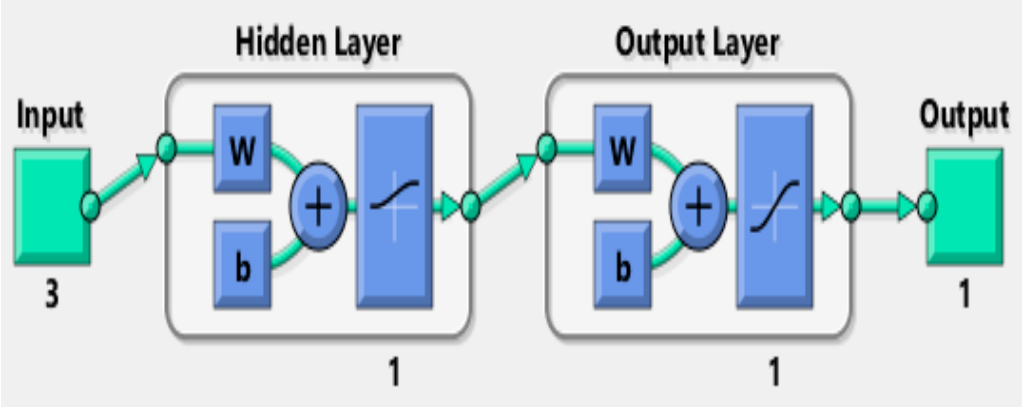

Figure 5. Neural network structure of BMN-LogSig-ANN-3-1-1.

Table 7. Modelling performances at different stages for predicting the reference evapotranspiration using Blaney–Morin–Nigeria and Hargreaves–Samani input parameters with LOGSIG function.

Model Architecture	No. of Epochs	Training			Testing			Validation			Overall		
		RMSE (mm/d)	R^2	d	RMSE (mm/d)	R^2	d	RMSE (mm/d)	R^2	d	RMSE (mm/d)	R^2	d
BMN-Logsig-ANN-3-1-1	165	0.00092	0.9664	0.991	0.00337	0.9435	0.994	0.000751	0.9797	0.985	0.00077	0.9649	0.991
BMN-Logsig-ANN-3-2-1	150	0.00106	0.9828	0.995	0.0049	0.9822	0.995	0.001035	0.9826	0.995	0.00089	0.9824	0.995
BMN-Logsig-ANN-3-3-1	**18**	**0.00035**	**0.9885**	**0.997**	**0.00329**	**0.9868**	**0.995**	**0.000177**	**0.9883**	**0.996**	**0.00029**	**0.9877**	**0.995**
HAG-Logsig-ANN-3-1-1	65	0.00342	0.8069	0.94	0.00796	0.7848	0.94	0.005076	0.8002	0.936	0.00286	0.8029	0.94
HAG-Logsig-ANN-3-2-1	45	0.00314	0.8796	0.965	0.00203	0.8787	0.97	0.002273	0.8985	0.966	0.00263	0.809	0.966
HAG-Logsig-ANN-3-3-1	15	0.00164	0.8468	0.955	0.00136	0.8335	0.964	0.000754	0.87	0.954	0.00137	0.8462	0.956

The TanSig transfer function generally yielded a superior performance compared to the LogSig function, particularly for models with three hidden layer neurons. Notably, the BMN-Tansig-ANN-3-3-1 model achieved the best validation performance, with a remarkably low RMSE of 0.000056 mm/day, a high R^2 of 0.9890, and a d value of 0.9960 (Table 8). As shown in Table 8, the R^2 values across all models ranged from 0.7968 to 0.9890, the RMSE values ranged from 0.005076 mm/day to 0.000056 mm/day, and the d values ranged from 0.9340 to 0.9960. Interestingly, even the network trained with only one neuron (BMN-Training-ANN-3-1-1) produced good results, suggesting a potentially effective correlation between the Blaney–Morin–Nigeria model parameters and the target Penman–Monteith values within the ANN framework. Overall, all models performed well with acceptable error levels (low RMSE) and high coefficients of determination (R^2). The estimated daily cassava crop evapotranspiration (ETc) remained consistent at approximately 2.3 mm/day across growth stages (1.2 mm/day for initial, 1.9 mm/day for developmental, 3.0 mm/day for mid-season, and 1.8 mm/day for late season).

Table 8. ANN model performance for predicting the reference evapotranspiration using Blaney–Morin–Nigeria and Hargreaves–Samani input parameters with TANSIG function over Cross River basin.

Model Architecture	No. of Epochs	Training			Testing			Validation			Overall		
		RMSE (mm/d)	R^2	d	RMSE (mm/d)	R^2	d	RMSE (mm/d)	R^2	d	RMSE (mm/d)	R^2	d
BMN-Tansig-ANN-3-1-1	38	0.0013	0.9652	0.991	0.0036	0.9464	0.994	0.0005	0.9793	0.986	0.0011	0.9644	0.99
BMN-Tansig-ANN-3-2-1	31	0.002967	0.98	0.995	0.001731	0.9705	0.996	0.000764	0.9889	0.991	0.002484	0.9795	0.994
BMN-Tansig-ANN-3-3-1	**22**	**0.000756**	**0.9883**	**0.997**	**0.002803**	**0.9876**	**0.997**	**0.000056**	**0.989**	**0.996**	**0.00063**	**0.9877**	**0.997**
HAG-Tansig-ANN-3-1-1	359	0.003225	0.8077	0.942	0.007716	0.7776	0.94	0.005076	0.7968	0.934	0.0027	0.8021	0.941
HAG-Tansig-ANN-3-2-1	13	0.003021	0.8361	0.949	0.006759	0.8149	0.958	0.002273	0.8572	0.946	0.002529	0.8354	0.95
HAG-Tansig-ANN-3-3-1	99	0.000231	0.8996	0.972	0.001108	0.8718	0.973	0.000754	0.9038	0.965	0.000193	0.8951	0.971

3.5. Comparison of Estimated Crop Evapotranspiration of Cassava (ETc) Using Artificial Neural Network (ANN) Models

Table 9 summarizes the estimated daily cassava crop evapotranspiration (ETc) values for various growth stages (initial, developmental, mid-season, and late season). The ETc values predicted by the ANN models strongly agreed with those obtained from the standard Penman–Monteith method, as evidenced by a low coefficient of variation (CV) of only 0.01%. This aligns with the findings of Gomes [29], who reported the effectiveness of CV in determining the variability of estimates. The Blaney–Morin–Nigeria model consistently underestimated ETc across all stages, while the Hargreaves–Samani model generally overestimated these values. Overall, the ANN models demonstrated superior accuracy in estimating daily cassava crop evapotranspiration compared to the traditional empirical methods (Blaney–Morin–Nigeria and Hargreaves–Samani models).

Table 9. Comparison of crop evapotranspiration of Cassava (ETc) using empirical models (Penman–Monteith model, Blaney–Morin–Nigeria model, and Hargreaves–Samani model) and Artificial Neural Network (ANN) models.

Growth Stages	Stage Length (Days)	Penman–Monteith (mm/d)	Hargreaves–Samani (mm/d)	Blaney–Morin–Nigeria (mm/d)	BMNT3-3-1 (mm/d)	BMNL3-3-1 (mm/d)	HAGT3-3-1 (mm/d)
Initial Stage	20	1.2	1.3	0.9	1.2	1.2	1.2
Developmental Stage	40	1.9	2.2	1.8	1.9	1.9	1.9
Mid-Season	90	2.9	3.4	2.8	3.0	3.0	3.0
Late Season	60	1.8	2.0	1.3	1.8	1.8	1.8
Total	210	2.2	2.6	2.0	2.3	2.3	2.3

3.6. Surplus or Deficit Water Requirement of Cassava as Estimated from ANN and the Empirical Models

Table 10 presents the average daily rainfall and potential water deficits/surpluses estimated by different models for each cassava growth stage; negative (-) values indicate water deficits, while positive (+) values represent periods of water surplus during the cropping season. During the initial stage, the mean daily rainfall was 3.5 mm, while all ANN and empirical models (except Blaney–Morin–Nigeria) estimated a slight excess rainfall (+2.3 mm) compared to crop evapotranspiration (ETc) needs. According to the Blaney–Morin–Nigeria and Penman–Monteith models, the developmental stage experienced lower rainfall (0.9 mm) and a water deficit of −1.0 mm. All ANN models estimated slightly lower deficits −1.0 mm, while the Hargreaves–Samani model estimated higher deficits (−1.3 mm). The mid-season displayed near-equilibrium conditions, with most models indicating a slight excess (+0.4 mm) except for the Hargreaves–Samani model (0.0 mm) and the Blaney–Morin–Nigeria model, which estimated a surplus (+0.6 mm). Finally, the late season received the highest rainfall (9.3 mm) with all models predicting a potential water surplus ranging from +7.4 mm (Hargreaves–Samani) to +8.0 mm (Blaney–Morin–Nigeria). These findings highlight the potential vulnerability of cassava during the developmental stage (particularly regarding water deficits). While Pereira et al. [33] classify cassava as

being tolerant to harsh conditions, other studies, such as those by Leon et al. [34,35] and Pacheco et al. [36], emphasize the importance of adequate moisture for sprouting and tuber formation during the initial and developmental stages. More et al. [37] and Daryanto et al. [38] further suggest that water deficits experienced within the first five months after planting (initial, developmental, and mid-season) can significantly reduce leaf number and size, shoot growth, and ultimately, root biomass. Therefore, for optimal cassava yield and production in the Cross River basin, it is crucial to address potential moisture deficits, particularly during the developmental stage.

Table 10. Surplus or deficit water requirement (ETc) of cassava in the Cross River basin.

Growth Stages	Stage Length (Days)	Rainfall (mm)	Penman–Monteith (mm/d)	Hargreaves–Samani (mm/d)	Blaney–Morin–Nigeria (mm/d)	BMN-Tansig-ANN- 3-3-1 (mm/d)	BMN-Logsig-3-3-1 (mm/d)	HAG-Tansig-3-3-1 (mm/d)
Initial Stage	20	3.5	+2.3	+2.3	+2.6	+2.3	+2.3	+2.3
Developmental Stage	**40**	**0.9**	−1.1	−1.3	−1.0	−1.0	−1.0	−1.1
Mid-Season	**90**	**3.4**	+0.5	0.0	+0.6	+0.4	+0.4	+0.4
Late Season	60	9.3	+7.5	+7.4	+8.0	+7.5	+7.5	+7.5

4. Conclusions

The Mann–Kendall test established an increasing rainfall trend during the cassava cropping season in the Cross River basin and a decreasing trend in cassava yield. The investigation encompassed the prediction of cassava crop evapotranspiration (ETc) with the training, validation, and testing of empirical and ANN models, using limited climatic data. The ANN models, particularly BMN-Tansig-ANN-3-3-1, BMN-Logsig-ANN-3-3-1, and HAG-Tansig-ANN-3-3-1, yielded more accurate ETc estimates (approximately 2.3 mm/day) with lower errors and higher values of Willmott's index of agreement compared to the standard Penman–Monteith method. These results were superior to those obtained from the Blaney–Morin–Nigeria and Hargreaves–Samani models. Notably, the variables used in the Blaney–Morin–Nigeria model proved more suitable for the Artificial Neural Network model predictions in comparison to the variables of the Hargreaves–Samani model. Furthermore, our analysis revealed the influence of increasing neuron number and transfer functions on prediction accuracy. The potential water deficits were identified during the developmental stage (approximately −1.1 mm/day) and mid-season (approximately −0.1 mm/day) can hinder root biomass production and overall cassava yield in the Cross River basin. This study highlights a water deficit during the developmental stage as a critical determinant in the reduction in cassava yield. Consequently, there is a pressing need to implement effective irrigation strategies to mitigate the adverse effects of climate change on cassava productivity and food security. The ANN framework employed in this study presents a promising approach for water requirement prediction to support such irrigation strategies.

Author Contributions: Investigation, O.O.E.; Data curation, O.O.E., O.T.F., I.E.O. and A.T.O.; Writing—original draft, O.O.E., T.B. and O.E.A.; Writing—review & editing, O.T.F. and O.E.A.; Supervision, O.T.F., M.A., A.E.A., P.O. and A.F. All authors have read and agreed to the published version of the manuscript.

Funding: This research received no external funding.

Data Availability Statement: The data presented in this study are available on request from the corresponding authors. The data are not publicly available due to personal reasons.

Conflicts of Interest: The authors declare no conflict of interest.

References

1. Stanhill, G. Evapotranspiration. In *Reference Module in Earth Systems and Environmental Sciences*; Elsevier: Amsterdam, The Netherlands, 2019.
2. Allen, R.G.; Pereira, L.S.; Raes, D.; Smith, M. *Crop Evapotranspiration: Guidelines for Computing Crop Water Requirements*; FAO Irrigation and Drainage Paper No 56. Food and Agriculture Organization, Land and Water; FAO: Rome, Italy, 1998.
3. Sretenka, S.; Zorica, S.; Ružica, S.; Nataša, Č.; Pavel, B.; Nada, R.; Milica, R.; Mladen, T. Assessment of Empirical Methods for Estimating Reference Evapotranspiration in Different Climatic Zones of Bosnia and Herzegovina. *Water* **2023**, *15*, 3065. [CrossRef]
4. Debnath, S.; Adamala, S.; Raghuwanshi, N.S. Sensitivity Analysis of FAO-56 Penman-Monteith Method for Different Agro-ecological Regions of India. *Environ. Process.* **2015**, *2*, 689–704. [CrossRef]
5. Izadifar, Z. Modeling and Analysis of Actual Evapotranspiration Using Data Driven and Wavelet Techniques. Master's Thesis, Department of Civil and Geological Engineering. University of Saskatchewan, Saskatoon, SK, Canada, 2010.
6. Food and Agriculture Organization of the United Nations (FAO). *Harmonized World Soil Data Base*; Version 1.2; Food Agriculture Organization: Rome, Italy, 2012.
7. Ahiakwo, A.A.; Isirima, C.B.; Inimgba, D.G. Appraisal and projection of cassava mash sieving technology. *Net J. Agric. Sci.* **2015**, *32*, 49–55.
8. Alatise, M.O. Fostering irrigation practices in the humid tropics of (South-western) Nigeria to sustain life and development. In Proceedings of the XVIIth World Congress of the International Commission of Agricultural Engineering (CIGR) Land and Water Engineering Conference CSBE100901, Québec, QC, Canada, 13–17 June 2010.
9. Isaiah, A.I.; Yamusa, A.M.; Odunze, A.C. Impact of Climate Change on Rainfall Distribution on Cassava Yield in Coastal and Upland Areas of Akwa Ibom State, Nigeria. *J. Exp. Agric. Int.* **2020**, *42*, 44–53.
10. Duru, J.O. Blaney-Morin-Nigeria evapotranspiration model. *J. Hydrol.* **1984**, *70*, 71–83. [CrossRef]
11. Akpabio, E.M.; Watson, N.M.; Ite, U.E.; Ukpong, I.E. Integrated water resources management in the Cross River Basin, Nigeria. *Int. J. Water Resour. Dev.* **2007**, *23*, 691–708. [CrossRef]
12. Akpan, E.A.; Udoh, V.S. Evaluation of Cassava (Manihot Esculenta crantz) genotype for yield and yield component, tuber bulking, early maturity in Cross River Basin flood plains, Itu, Akwa Ibom State, Nigeria. *Can. J. Agric. Crops* **2017**, *2*, 68–73.
13. Sarangi, A.; Madramootoo, C.A.; Enright, P.; Prasher, S.O.; Patel, R.M. Performance evaluation of ANN and geomorphology-based models for runoff and sediment yield prediction for a Canadian watershed. *Curr. Sci.* **2005**, *89*, 2022–2033.
14. Mann, H.B. Non-Parametric Test against Trend. *Econometrica* **1945**, *13*, 245–259. [CrossRef]
15. Kendall, M.G. The Treatment of Ties in Ranking Problems. *Biometrika* **1945**, *33*, 297–298. [CrossRef]
16. Hisdal, H.; Stahl, K.; Tallaksen, L.M.; Demuth, S. Have streamflow droughts in Europe become more severe or frequent. *Int. J. Climatol.* **2001**, *21*, 317–333. [CrossRef]
17. Wu, H.; Soh, L.K.; Samal, A.; Chen, X.H. Trend analysis of streamflow drought events in Nebraska. *Water Resour. Manag.* **2008**, *22*, 145–164. [CrossRef]
18. Koudahe, K.; Kayode, A.; Samson, A.; Adebola, A.; Djaman, K. Trend Analysis in Standardized Precipitation Index and Standardized Anomaly Index in the Context of Climate Change in Southern Togo. *Atmos. Clim. Sci.* **2017**, *7*, 401–423. [CrossRef]
19. Akpan, E.A.; Ikeh, A.O. Growth and yield response of cassava (Manihot esculenta Crantz) varieties to different spacing in Uyo, Southsouthern Nigeria. *J. Agric. Crop Res.* **2018**, *6*, 19–27.
20. Hargreaves, G.H.; Samani, Z.A. Reference Crop Evapotranspiration from Temperature. *Appl. Eng. Agric.* **1985**, *1*, 96–99. [CrossRef]
21. Rahsepar, M.; Mahmoodi, H. Predicting Weekly Discharge Using Artificial Neural System (ANN) Optimized by Artificial Bee Colony (ABC) Algorithm: A Case Study. *Civ. Eng. Urban Plan. Int. J. (CiVEJ)* **2014**, *1*, 1–13.
22. ASCE. Artificial neural networks in hydrology. I: Preliminary concepts. *J. Hydrol. Eng.* **2000**, *5*, 115–123. [CrossRef]
23. Fojnica, A.; Osmanoviæ, A.; Badnjeviæ, A. Dynamical model of tuberculosis-multiple strain prediction based on artificial neural network. In Proceedings of the 2016 5th Mediterranean Conference on Embedded Computing (MECO), Piscataway, NJ, USA, 12–16 June 2016; IEEE: Piscataway, NJ, USA, 2016; pp. 290–293. [CrossRef]
24. Anifowose, F.A.; Labadin, J.; Abdulraheem, A. Hybrid intelligent systems in petroleum reservoir characterization and modeling: The journey so far and the challenges ahead. *J. Pet. Explor. Prod. Technol.* **2017**, *7*, 251–263. [CrossRef]
25. Singh, J.; Vernon Knapp, H.; Arnold, J.G.; Demissie, M. Hydrologic modeling of the Iroquois River watershed using HSPF and SWAT. *J. Am. Water Resour. Assoc.* **2005**, *41*, 343–360. [CrossRef]
26. Chicco, D.; Warrens, M.J.; Jurman, G. The coefficient of determination R-squared is more informative than SMAPE, MAE, MAPE, MSE and RMSE in regression analysis evaluation. *PeerJ Comput. Sci.* **2021**, *7*, e623. [CrossRef]
27. Willmott, C.J.; Robeson, S.M.; Matsuura, K.; Ficklin, D.L. Assessment of three dimensionless measures of model performance Environ. *Modell. Softw.* **2015**, *73*, 167–174. [CrossRef]
28. Ewona, I.O.; Udo, S.O. Climatic condition of Calabar as typified by some meteorological parameters. *Glob. J. Pure Appl. Sci.* **2010**, *17*, 81–86.
29. Gomes, F.P. *Curso de Estatística Experimental*, 15th ed.; Esalq: Piracicaba, Brazil, 2009; p. 477, ISBN 9788571330559.

30. Blenkinsop, S.; Fowler, H.J.; Barbero, R.; Chan, S.C.; Guerreiro, S.B.; Kendon, E.; Lenderink, G.; Lewis, E.; Li, X.-F.; Westra, S.; et al. The INTENSE project: Using observations and models to understand the past, present and future of subdaily rainfall extremes. *Adv. Sci. Res.* **2018**, *15*, 117–126. [CrossRef]
31. Sun, Q.X.; Zhang, F.W.; Zwiers, S.; Westra, L.V.; Alenxander, L.V. A global, continental and regional analysis of changes in extreme precipitation. *J. Clim.* **2021**, *34*, 243–258. [CrossRef]
32. Donat, M.G.; Lowry, A.L.; Alexander, L.V.; O'Gorman, P.A.; Maher, N. More extreme precipitation in the world's dry and wet regions. *Nat. Clim. Chang.* **2016**, *6*, 508–513. [CrossRef]
33. Pereira, L.F.M.; Zanetti, S.; Silva, M.A. Water relations of Cassava cultivated under water-deficit levels. *Acta Physiol. Plant.* **2018**, *40*, 13. [CrossRef]
34. León, R.; Pérez, M.; Fuenmayor, F.; Gutiérrez, M.; Rodríguez, A.; Rodríguez, G.Y.; Marín, C. Evaluación fisiológica y agronómica de clones promisorios de yuca (Manihot esculenta Crantz) sometidos a condiciones de estrés por sequía. *Rev. UNELLEZ Cienc. y Tecnol.* **2016**, *34*, 50–57.
35. León, R.; Pérez, M.; Fuenmayor, F.; Rodríguez, A.; Rodríguez, G.Y.; Marín, C. Calidad de las raíces en cuatro clones de yuca (Manihot esculenta Crantz) y efecto del régimen de riego. *Bioagro* **2018**, *30*, 87–91.
36. Pacheco, R.I.L.; Macias, M.P.; Campos, F.C.F.; Izquierdo, A.J.R.; Izquierdo, G.A.R. Agronomic and physiological evaluation of eight cassava clones under water deficit conditions. *Revisit. Fac. Agron.* **2020**, *73*, 9109–9119. [CrossRef]
37. More, S.J.; Bardhan, K.; Ravi, V.; Pasala, R.; Chaturvedi, K.A.; Lal, M.K.; Siddique, H.M. Morphophysiological Responses and Tolerance Mechanisms in Cassava (*Manihot esculenta* Crantz) Under Drought Stress. *J. Soil. Sci. Plant Nutr.* **2023**, *23*, 71–91. [CrossRef]
38. Daryanto, S.; Wang, L.; Jacinthe, P.A. Global synthesis of drought effects on cereal, legume, tuber and root crops production: A review. *Agric. Water Manag.* **2017**, *179*, 18–33. [CrossRef]